

**Electromagnetic Interferences between Large Power Systems and Pipelines
by using a Multizone Soil Model**

Nihar Raj(a), Roberto Andolfato(b), Daniele Cuccarollo(b)
(a) ABB India Ltd - India
(b) SINT Ingegneria - Italy

SUMMARY

This work relates with the frequency domain module XGSA_FD of the XGSLab® simulation environment [12], [13] which allow many applications of practical interests and in particular the analysis of electromagnetic interference between above and underground power systems and aerial or buried pipelines in a very realistic way.

The XGSLab® solver is based on Maxwell equations and Sommerfeld integrals and can be applied for the solution of both aerial and underground conductors network taking into account the earth effects in the frequency domain between from DC condition up to a few MHz. Original algorithms have been developed for solving an hybrid method which takes into account transmission line, circuit and electromagnetic theory combined into a single integrated calculation model considering the effects of self impedance, resistive, capacitive and inductive coupling, soil parameters frequency dependence and propagation effects.

In the first theoretical part, a synthetic description of the implemented method is given together with its application limits and range.

The second part of the paper introduces the multi-zone soil model; a model, which is very useful in case of large power systems (big power plants, big switchyards like AIS, GIS hybrid technology till 1200 kV system). It is also observed that soil resistivity readings in the big locations are also taken at multiple locations thus making it more close to the realistic condition.

The third part of the paper describes separately the effects of conductive and inductive interferences between power systems and pipelines.

The fourth part of the paper is devoted to the description of a specific study case, which was reckoned the best way for assessing the capabilities of the proposed approach. The study case is related to the electromagnetic interference between a power line under faulty conditions and a buried pipeline, including the effects of a substation grounding system. The interference

effects then include contemporary both conductive and inductive coupling effects. It is then shown how it is possible to perform realistic simulations of increasingly frequent problems of electromagnetic interference in even complex scenarios.

Finally, unlike classical finite elements methods, it is worth noticing that the hybrid approach requires limited CPU power and RAM resources and even if they have room for improvement, they are already adequate for most engineering applications.

KEYWORDS

Electromagnetic Interferences, Grounding Systems, Pipelines, Computer Modelling, Hybrid Method, PEEC.

1 - INTRODUCTION

The large improvement of power computing performances is contributing to the diffusion of calculation programs for electromagnetic simulations taking into account realistic condition and in particular the earth effects.

These programs have many engineering applications, as for instance:

- Grounding Systems
- Cathodic Protection Systems
- Electromagnetic Fields
- Electromagnetic Interferences
- Fault Currents Distribution
- Lighting Protection Systems

Each application has specific needs as for example concerns a different frequency range. As known, with increasing frequency the possible approximations are less and less and the calculation model is becoming increasingly complex. For instance, when frequency increases, mutual coupling, soil parameters frequency dependence and propagation delay cannot be neglected.

One of the most promising and effective calculation model in the frequency range between DC to a few MHz is the “Partial Element Equivalent Circuit (PEEC)” method that in the following for historical reasons or for tradition in the grounding community we prefer to call “hybrid method”.

Calculation models for electromagnetic simulations including the earth effects may be based on following different approaches: 1) Electromagnetic field theory; 2) Transmission line theory; 3) Hybrid methods, 4) Circuit theory. This classification is not rigorous as indicated in [9], but is generally adopted in the literature. For a comprehensive overview on these kind of computational methods refer to [9].

Hybrid methods consider transmission line, circuit and electromagnetic field theory combined into a single model, and are often preferred in the frequency range of interest. Hybrid methods are very useful for engineering purposes because they are accurate and flexible, and can allow an easy way to include additional external parameters such as electromotive forces, currents, and impedances [10].

In the following paper the calculation were performed by XGSA_FD® a module of the software package XGSLab®. This program is based on an hybrid method and on the main assumptions listed in Tab. 1.1.

Resistive Coupling	Yes
Capacitive Coupling	Yes
Self-Impedance	Yes
Inductive Coupling	Yes
Soil Parameters	$\rho, \varepsilon = f(\omega)$
Propagation Law	$e^{-\gamma r/r}$

Tab 1.1. Aspects taken into account in the used program.

2 – HYBRID METHOD

In the following, a short description of the hybrid method implemented in the used program is provided.

The implemented method can solve conductors network in the 3D space and including sources (conductors with current and voltages known), and victims (conductors with current and voltages unknown). The conductors network is partitioned into small finite elements (current and charge cells), and then, the electromagnetic field and transmission line theories are used to calculate the circuit parameters, whereas circuit theory is employed to describe the relations among parameters such as voltages and currents and the metallic connections among elements. All conductors of the system have to be thin enough in order to be simulated with a suitable number of thin and straight elements.

The implemented method derives directly from the Maxwell equations. Using the scalar and vector potentials, Maxwell equations [2] can be written as in the following (Helmholtz equations):

$$\begin{cases} \Delta \dot{\mathbf{A}} - \dot{\gamma}^2 \dot{\mathbf{A}} = -\mu \dot{\mathbf{J}} \\ \Delta \dot{V} - \dot{\gamma}^2 \dot{V} = -\frac{\dot{q}}{\dot{\epsilon}} \end{cases} \quad (2.1)$$

where $\dot{\gamma} = \sqrt{j\omega\mu(\sigma + j\omega\epsilon)}$ represents the propagation coefficient of the medium and \dot{q} and $\dot{\mathbf{J}}$ represent charge and current density distribution on the sources respectively.

Solution of (2.1) for sources with linear current and charge density distribution are given by the following equations:

$$\begin{cases} \dot{\mathbf{A}} = \frac{\mu}{4\pi} \int_L \frac{\dot{\mathbf{j}} e^{-\dot{\gamma}r}}{r} dl \\ \dot{V} = \frac{1}{4\pi\dot{\epsilon}} \int_L \frac{\dot{q} e^{-\dot{\gamma}r}}{r} dl \end{cases} \quad (2.2)$$

Maxwell equations give the following well known relation between electric field and scalar and vector potentials:

$$\dot{\mathbf{E}} = -\text{grad}\dot{V} - j\omega\dot{\mathbf{A}} \quad (2.3)$$

Taking into account that the electric field and vector potential on the surface of a conductor are parallel to the conductor axis [4], only the magnitude of vectors in (2.3) need to be considered and (2.3) written along the conductor axis gives:

$$\dot{E} = -\frac{\partial \dot{V}}{\partial l} - j\omega\dot{A} \quad (2.4)$$

On the other hand, the tangential electric field on the surface of a conductor, taking into account their self impedance, gives:

$$\dot{E} = z\dot{I} \quad (2.5)$$

Combining (2.4) and (2.5), the following fundamental differential equation is obtained:

$$z\dot{I} + j\omega\dot{A} + \frac{\partial \dot{V}}{\partial l} = 0 \quad (2.6)$$

Equation (2.6) is derived directly from the Maxwell equations and is then valid in all conditions (also non stationary). In practical cases, (2.6) can be solved only in a numerical way. The conductors network is then partitioned into a suitable number of short elements. Each element is oriented between its start point (in) and its end point (out). Integrating (2.6) between the ends of an element, replacing the vector and scalar potential with (2.2) and rearranging, the following linear equation is obtained:

$$\dot{Z}_i \dot{I}_i + \sum_{j \neq i} \dot{M}_{ij} \dot{I}_j + \sum (\dot{W}_{outij} - \dot{W}_{inij}) \dot{J}_j = 0 \quad (2.7)$$

with:

$$\dot{M}_{ij} = \frac{j\omega\mu}{4\pi} \int_{in}^{out} \int_{in}^{out} \frac{e^{-\gamma r}}{r} dl_i dl_j$$

$$\dot{W}_{outij} = \frac{\dot{\rho}}{4\pi l} \int_{in}^{out} \frac{e^{-\gamma r}}{r} dl_j \Bigg|_{out}$$

$$\dot{W}_{inij} = \frac{\dot{\rho}}{4\pi l} \int_{in}^{out} \frac{e^{-\gamma r}}{r} dl_j \Bigg|_{in}$$

and where \dot{Z} represents the self impedance of the element, \dot{M} and \dot{W} represent partial mutual coupling and partial potential coefficients between elements respectively, and \dot{I} and \dot{J} represent longitudinal and leakage currents respectively.

Writing a linear equation for each element, the Maxwell equations are then reduced to a linear system. For the calculation of the linear system coefficients and then of the self and partial mutual coupling and partial potential coefficients between elements, the formulas in [1], [3], [5] the shifting complex images method (SCIM) [8] and the modified images method (MIM) [7] has been used respectively. If these coefficients are calculated taking into account the propagation delay, the resulting model is a full-wave hybrid method.

Each element is represented with a simplified T equivalent circuit as shown in Fig. 2.1 and introduces the following unknowns:

- Input and Output currents I_{in} and I_{out}
- Leakage current J
- Potential V of the middle point

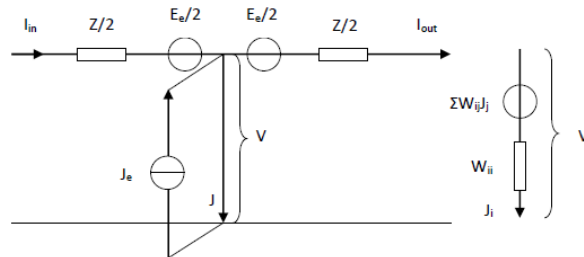


Fig. 2.1. Equivalent circuit of each element

The resulting linear systems can be written as follows:

$$\begin{cases} \{V\} = [W]\{J\} \\ \{E_z\} + \{E_e\} = -([Z] + [M])\{I\} \\ \{J\} = [A]\{I\} + \{J_e\} \end{cases} \quad (2.8)$$

where:

- $[W]$ = matrix of self and mutual partial potential coefficient
- $[Z]$ = matrix of self-impedances
- $[M]$ = matrix of partial mutual impedances
- $[A]$ = incidence matrix which expresses the elements connectivity
- $\{V\}$ = array of potentials
- $\{I\}$ = array of currents
- $\{J\}$ = array of leakage currents
- $\{E_z\}$ = array of voltage drops
- $\{E_e\}$ = array of forcing electromotive force
- $\{J_e\}$ = array of injected currents

The linear system (2.8), provides the distributions of currents, potentials and leakage currents along the victims taking into account the influence of eventually sources. From these main results, it is possible to calculate other important distributions as for instance:

- Earth surface potentials and then Touch and Step Voltages
- Electric Fields
- Magnetic Fields

The calculation model above described is suitable for the “frequency domain” but also in the “time domain” by using the direct and inverse Fourier transform. As known a time domain transient $s(t)$ can be considered as a superposition of many single frequency signals as follows:

$$s(t) = \sum_{n=-\infty}^{\infty} \dot{S}_n e^{j2\pi nft} \quad (2.9)$$

where:

- \dot{S}_n = magnitude of the n^{th} harmonic
- f = base frequency

The \dot{S}_n values can be calculated by using a direct Fourier transform. In practical cases the maximum harmonics number in (2.9) is limited to a value N depending on the frequency spectrum of the input transient. The above described frequency domain model can be used for each harmonic and, at the end, N different output in the frequency domain will be obtained. The time domain output can be obtained from these outputs by using the inverse Fourier transform.

This described process in general could be time consuming but it can be speeded up by limiting the harmonics to a reduced number of critical frequencies.

3 – SOIL MODELS

The soil electromagnetic properties include resistivity, permittivity and permeability.

The soil permeability can normally be regarded as equal to the vacuum permeability.

The soil resistivity and permittivity depend from moisture, temperature and chemical content, and are also frequency dependant. There is no a generally accepted formulation to express the frequency dependence of soil parameters but anyway, at power frequency (than at low frequency), soil permittivity effects may be surely neglected and soil resistivity can be approximated with its DC value.

XGSLab can consider the frequency dependence of soil parameters according to different models (Messier, Visacro – Portela, Visacro – Alipio ...) but in the following, taking into account the

frequencies of interests, the soil parameters will be considered frequency independent and the low frequency soil resistivity will be adopted.

The soil resistivity value is liable to great variations.

The ranges of variations of the soil resistivity are following:

- Exceptionally low values: from 1 up to 10 Ωm
- Usual Values: from 10 up to 1000 Ωm
- Exceptionally High Values: from 1000 up to 10000 Ωm

As said, the soil resistivity depends on the environmental conditions and then it is not possible to assign a single value for the resistivity of a soil material. For this reason the resistivity value must not be obtained from literature or tables but must be measured. The only reliable data are those related to the specific site.

The Wenner four-pin method is the most commonly used technique for soil resistivity measurements. As known, for each site, resistivity measurements should be done using different probe distances in order to investigate how resistivity change with depth, and in different places in order to investigate how resistivity change in horizontal direction.

Then, resistivity measurements values have then be analysed and this operation can be not trivial.

In fact, in practical cases, the distribution of the soil resistivity measurements is often as represented in Fig. 3.1.

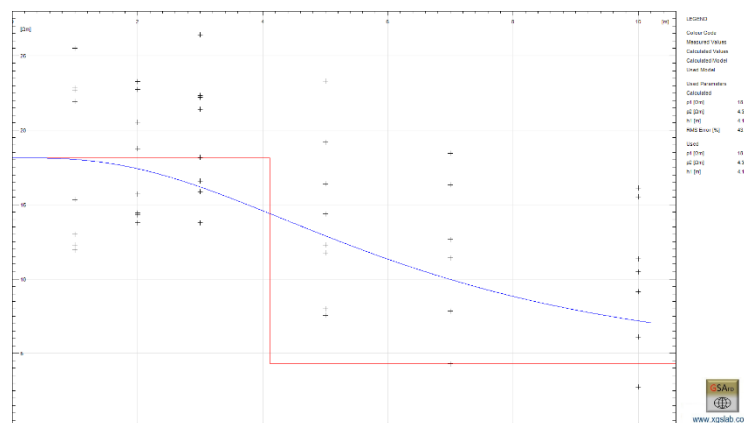


Fig. 3.1. Measured resistivities (black crosses) and equivalent double layer model (blue and red lines)

Generally speaking, the soil model choice is difficult mainly for the following reasons:

- The resistivity of the upper layer changes with temperature, rain, pollution ...
- The resistivity of the deep layers changes mainly with the kind of soil
- In case of large sites, horizontal resistivity variations is unavoidable
- In case of large sites, the soil surface often cannot be considered flat

In practical cases, the following rules can be adopted:

- A uniform soil assumption is often unacceptable or acceptable only for preliminary evaluations
- In case of small and medium systems, a double layer soil model represents an acceptable approximation in most cases (this is because touch and step voltages depend mainly on the upper layer resistivity and the resistance to earth depends on the bottom layer resistivity and using a double layer soil model both conditions can be fit)
- In case of small systems, a more sophisticated soil model (for instance a multilayer soil model) could be useful but only if the horizontal resistivity variations are negligible
- In case of large systems, experience shows the horizontal resistivity variations are unavoidable (and in some cases it is also difficult to assume the flat surface of the soil). The use of a multilayer soil model can improve the soil model only in some specific points but not in general. In these cases, the use of a multizone soil model represents often the preferable solution
- All models provide a good approximation only close to the measurement places

With the multizone soil model the soil can be assumed divided in more zones as in Fig. 3.2. Each zone can be represented with a uniform soil model. A more refined soil model for each single zone is impracticable and anyway, also with a uniform soil model the solution is rigorous with two zones while, with more zones can be found only in an approximate way and under certain conditions. In particular, conductors should be not close to the intersection between three or more zones. Bare elements in the orange areas in Fig. 3.1 must be avoided (the radius of the orange areas is a few dozen meters).

Taking into account the limitations of the soil models, it is easy to understand the reason why the use of a more sophisticated electric model of the conductors network, for instance a model which takes into account self and mutual impedances effects, is preferable to attempt to improve the soil model. In fact, the circuit parameters can be known better than the soil resistivity value.

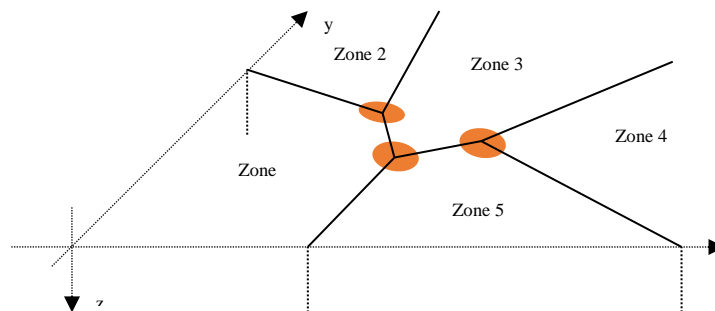


Fig. 3.2. Multizone Soil Model

4 – ELECTROMAGNETIC INTERFERENCES

Metal pipelines, for part of their length, may be exposed to several types of influences of near high voltage substations or power lines. These influences can result of three types of couplings:

- Capacitive
- Inductive
- Conductive

Capacitive coupling occurs only for aerial pipelines close to high voltage aerial power lines and in the following will be neglected (anyway XGSLab may consider also this condition).

The electromagnetic interferences among substations or power lines and buried pipeline are due mainly to the conductive and inductive coupling respectively and can give hazardous situation for people or damage to the pipeline or to the connected equipment.

Conductive effects occurs only in case of fault to earth conditions and cause a potential rise of the pipeline and of the neighbouring soil with regard to the remote earth. As known, the conductive effects grow with the current to earth and with the soil resistivity and decrease with the distance between substations and pipeline.

Inductive effects occurs in both steady state and fault conditions and cause an electromotive force along the pipeline and, as consequence, also longitudinal currents, leakage currents and potentials distributions. The inductive effects grow with the power line current, with the parallelism length, with the soil resistivity and decrease with the distance between power line and pipeline.

Smaller inductive effects appear under steady state conditions while significant induced voltages appear under faulty conditions and in particular under single phase to earth fault condition. On the other hand, permissible induced voltages established by the standards are different for steady state and fault conditions. For these reasons, the electromagnetic interferences between power line and pipeline have to be evaluated in both steady state and faulty conditions.

The conductive effects among a substation grounding system and an insulated and infinite length pipeline are represented in a qualitative way in Fig. 4.1, 4.2, 4.3 and 4.4. The grid size is 100 x 100 m with meshes 10 x 10 m and depth 1 m and the pipeline is as described in 5. The distance between pipeline and grid is 10 m. The current injected in the earth is 10 kA 50 Hz and the soil model is uniform with resistivity 100 Ωm and relative permittivity 10. The potential rise along the pipeline is highest in the point closest to the substation and then decrease. The longitudinal and leakage currents along the pipeline show that the pipeline picks up current from the ground near the substation and return it to the remote earth.

The inductive effects among an high voltage aerial pipeline and an insulated and infinite length pipeline are represented in a qualitative way in Fig. 4.5, 4.6, 4.7 and 4.8. The parallelism between power line and pipeline is 100 m and the pipeline is as described in 5. The horizontal and vertical distance between pipeline and grid is 10 m and 2 m respectively. The current along the power line is 10 kA 50 Hz and the soil model is uniform with resistivity 100 Ωm and relative permittivity 10. The induced electromotive force along the pipeline is due to the part of the power line parallel to the pipeline (the two parts orthogonal do not give contributions). Potential and current distributions are a consequence of the induced electromotive force and in case of well insulated pipeline may remain for long pipeline spans.

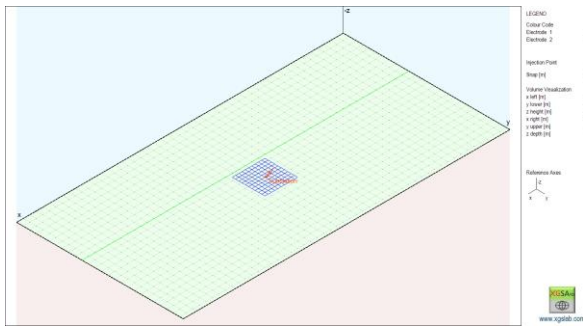


Fig. 4.1. Layout of substation (blue) and pipeline (green)

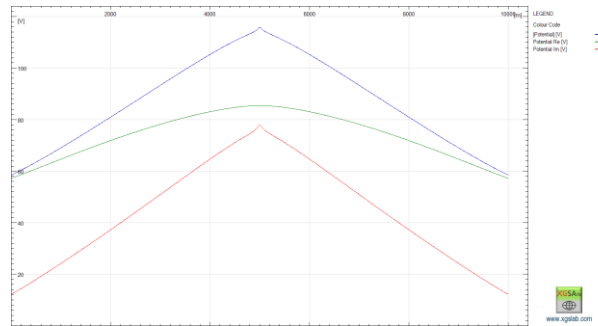


Fig. 4.2. Potential distribution along 10 km of pipeline (blue = Mod, green = Re, red = Im)

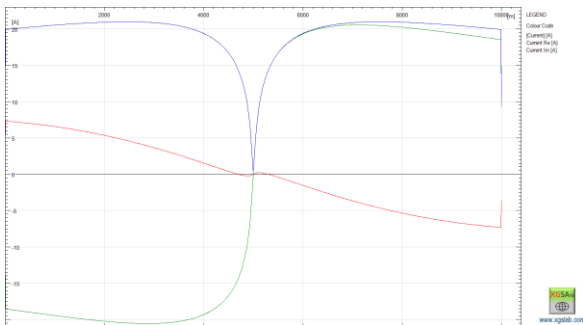


Fig. 4.3. Longitudinal current distribution along 10 km of pipeline (blue = Mod, green = Re, red = Im)

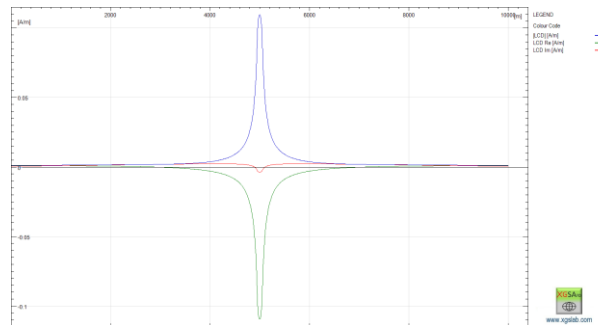


Fig. 4.4. Leakage current distribution along 10 km of pipeline (blue = Mod, green = Re, red = Im)

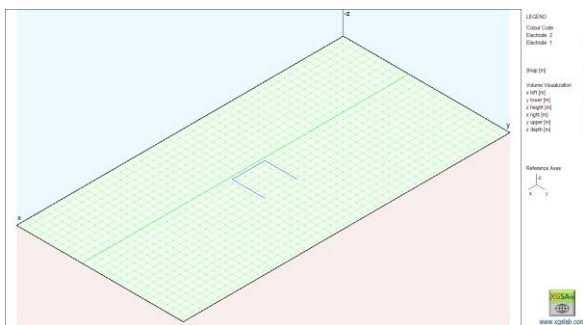


Fig. 4.5. Layout of power lines (blue) and pipeline (green)

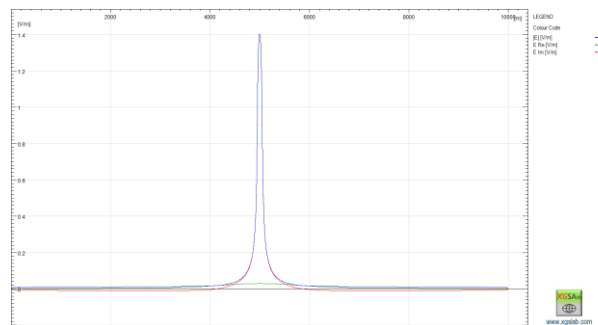


Fig. 4.6. Electromotive force distribution along 10 km of pipeline (blue = Mod, green = Re, red = Im)

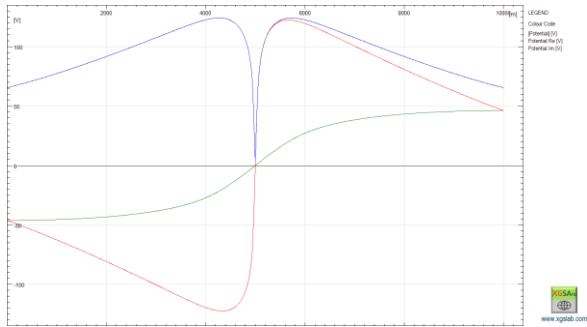


Fig. 4.7. Potential distribution along 10 km of pipeline (blue = Mod, green = Re, red = Im)

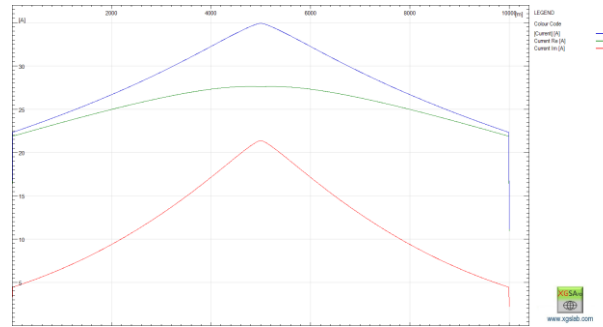


Fig. 4.8. Current distribution along 10 km of pipeline (blue = Mod, green = Re, red = Im)

The effects of the electromagnetic interferences can be calculated with formulas only with simplified layout and uniform or horizontally layered soil model. In cases of practical interests (complex layout, networks of power systems or pipelines, non-uniform soil model ...), these effects can be calculated only with a specific software.

The difficulty grows if moreover both conductive and inductive effects occur contemporary. This conditions will be considered in the following case study.

5 – CASE STUDY

As example, the electromagnetic interferences between a distribution substation 400/220 kV, two overhead power lines 400 kV, two overhead power lines 220 kV and an underground pipeline network are evaluated.

The layout of the system of conductors is shown in Figure 5.1 and Figure 5.2.

In order to consider a more realistic case, a contemporary conductive and inductive interference is considered. The main goal is to calculate the induced electromotive force (EMF), currents and voltages along the pipeline in case of a single phase to earth fault at the substation.

The interference zone is quite large and for this reason a multizone soil model with the following soil resistivity and relative permittivity has been considered (see soil zones border in Figure 5.1):

- Zone 1: $\rho = 100 \Omega\text{m} - \epsilon_r = 6$
- Zone 2: $\rho = 150 \Omega\text{m} - \epsilon_r = 6$
- Zone 3: $\rho = 80 \Omega\text{m} - \epsilon_r = 6$
- Zone 4: $\rho = 170 \Omega\text{m} - \epsilon_r = 6$
- Zone 5: $\rho = 220 \Omega\text{m} - \epsilon_r = 6$

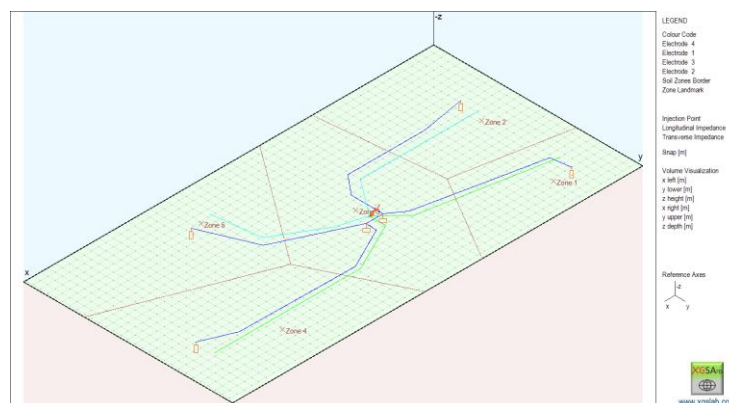


Figure 5.1: Layout of substation, power lines 400 kV (green), 220 kV (azure) and pipeline (blue)

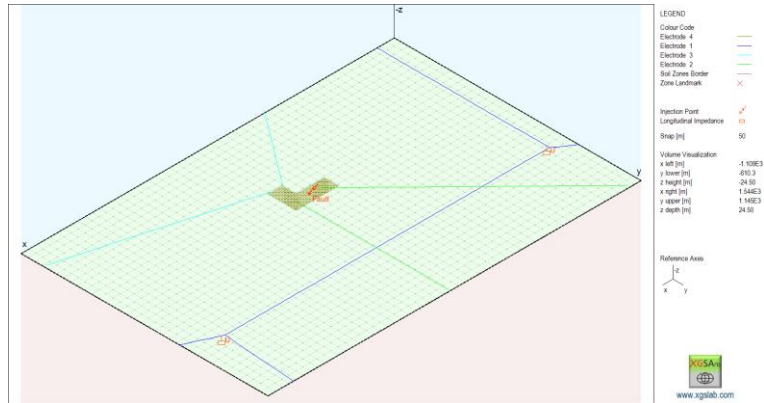


Figure 5.2: Detail of the substation grounding system layout

Only the pipeline incoming the zone of influence of the power system is taken into account. Based on [6], the width of the zone of influence can be calculated as follows:

$$d = 200\sqrt{\rho} \quad (5.1)$$

where:

- ρ (Ωm) = soil resistivity

The zone of influence in the specific case, varies in the range between 1789 and 2966 m.

The substation representation is limited to its grounding system layout.

The overhead power lines representations are simplified and takes into account only the phase conductors closest to the pipeline. The overhead earth wire screening effects are included in the calculation by applying a reduction factor “r” to the phase to earth fault current. The reduction factor depends on the number and self impedances of the overhead wires and on the mutual impedance between overhead wires and phase conductors and it is usually in the range 0.6 – 1.0.

$$r = \frac{I_e}{I_f} \quad (5.2)$$

where:

- I_e (A) = current to earth

- I_f (A) = fault current

In general conditions, XGSLab may consider complex scenarios. In particular, it is possible to simulate the overhead earth wire and also the effects of the tower lattice grounding systems but this is beyond the scope of this paper.

Other main data as in the following.

Power line 400 kV:

- $V = 400$ kV

- $f = 50$ Hz

- $h = 18$ m (average height of the lowest phase conductor)

- $I_f = 12.0$ kA \perp 30.0 deg (single phase to earth fault current)

- $r = 0.7$ (reduction factor)

- $t_f = 0.35$ s (clearance time)

Power line 220 kV:

- $V = 220$ kV

- $f = 50$ Hz
- $h = 15$ m (average height of the lowest phase conductor)
- $I_f = 8$ kA $\angle 0.0$ deg (single phase to earth fault current)
- $r = 0.8$ (reduction factor)
- $t_f = 0.35$ s (clearance time)

XGSLab may consider also the catenary of the aerial power line but similar refinements are usually not considered in the electromagnetic interference evaluations.

The fault current direction in all cases are towards the substation.

The current to earth in the substation is then:

$$I_e = 28.61 \text{ kA} \angle 17.07 \text{ deg}$$

Pipeline:

- Layout: infinite length in all directions and an insulating joint where indicate
- Insulating joint: protected by a surge protection device with a low frequency discharge voltage 350 V
- $h = 1.5$ m (axis depth)
- $d = 300$ mm (outer diameter excluding covering)
- $t = 9.5$ mm (metal wall thickness)
- $\rho_m: 1.7 \cdot 10^{-7} \Omega\text{m}$ (steel)
- $\mu_m: 300$
- $t_c = 2.5$ mm (covering thickness)
- $\rho_c: 10^7 \Omega\text{m}$ (polyethylene)
- $\epsilon_{rc}: 2.3$

The infinite length condition of the pipelines has been simulated with a transverse impedance corresponding to their characteristic impedances (at 50 Hz) $Z_c = 2.85 + j2.13 \Omega$.

The potential distribution calculate along the pipeline has to be compared with the permissible voltage. Usually Standards consider a permissible voltage for safety conditions of people and a different limit in order to avoid damage to the pipeline.

In fault conditions, Standard limits for safety conditions of people depend on the fault duration (for instance 1000 V if fault duration time is 0.35 s). This limits are referred to accessible metal parts.

The European standard limit (EN 50443 2012) in order to avoid damage to the pipeline in fault condition is 2000 V. This limit is referred to all parts.

The results of the interference are represented in the following Figures.

Figure 5.3 and Figure 5.4 represent the EMF and potential distribution respectively along a network of pipes and the discontinuities are related also to the kind of representation that appends all the pipes.

In the first stage calculation, the surge protection devices applied to the insulating joints are assumed not triggered. In this condition the difference between the potentials on the insulating joints are 1166 and 999 V and then well above the low frequency discharge voltage (350 V).

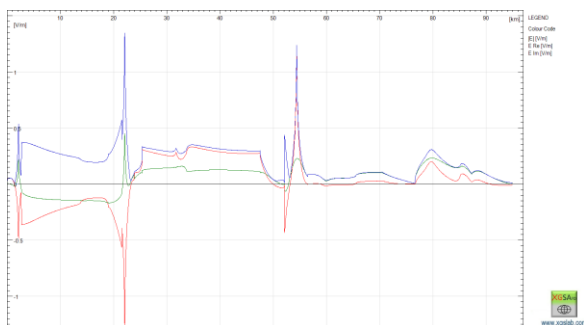


Figure 5.3: EMF distribution on pipeline with surge protection device not triggered

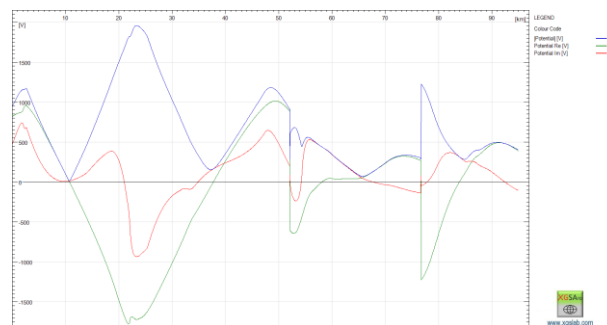


Figure 5.4: Potential distribution on pipeline with surge protection device not triggered

In the second stage calculation, the surge protection devices are assumed triggered.

Figure 5.5 indicates that the induced potentials on pipeline are higher than the permissible values for safety conditions of people (1000 V).

As mitigation measure, four additional resistances to earth (2.8Ω the central ones and 10Ω the lateral ones) are applied to the pipeline in the spans around the highest potentials points. These earth resistances (indicate as Ra in Figure 5.6), in steady state condition are not active because connected to the pipeline via surge protection devices.

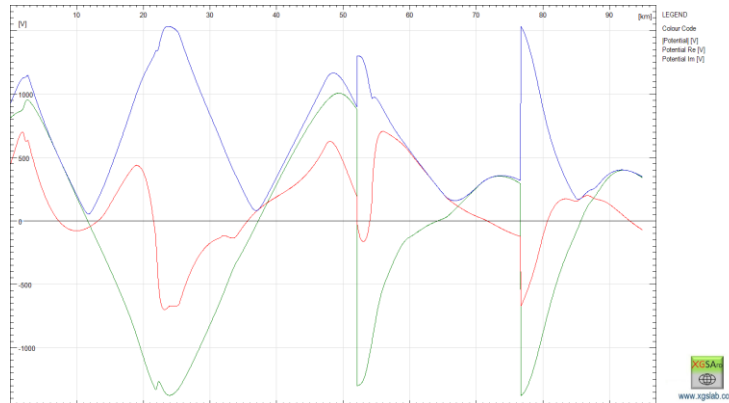


Figure 5.5: Potential distribution on pipeline with surge protection device triggered

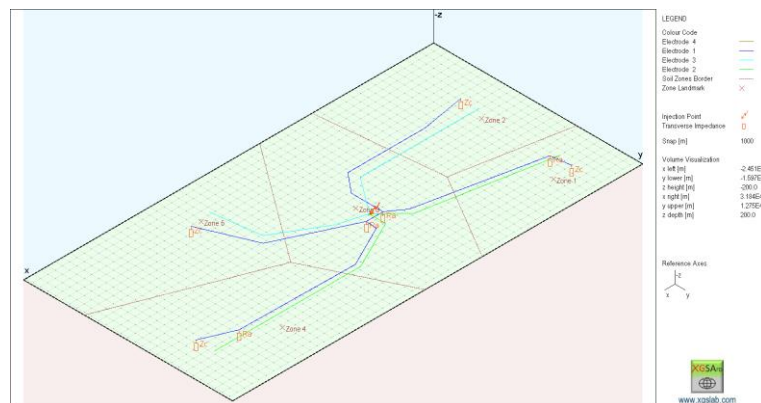


Figure 5.6: General layout with location of additional pipeline earthing

In the third stage calculation, the surge protection devices of insulating joints and of pipeline earthing are assumed triggered. Figure 5.9 indicates that the induced potentials are lower than the permissible values for safety conditions of people (1000 V). Figure 5.10 indicates that the covering stress voltage is lower than the limit in order to avoid damage to the pipeline (2000 V).

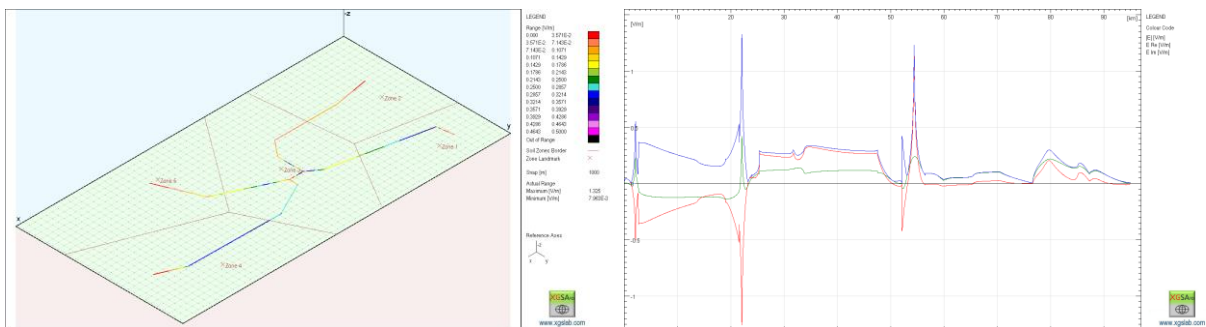


Figure 5.7: EMF distribution on pipeline with additional earthing

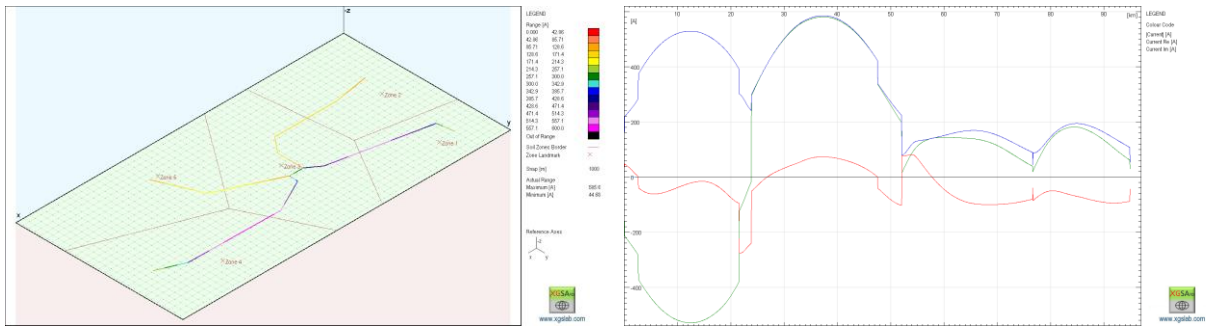


Figure 5.8: Current distribution on pipeline with additional earthing

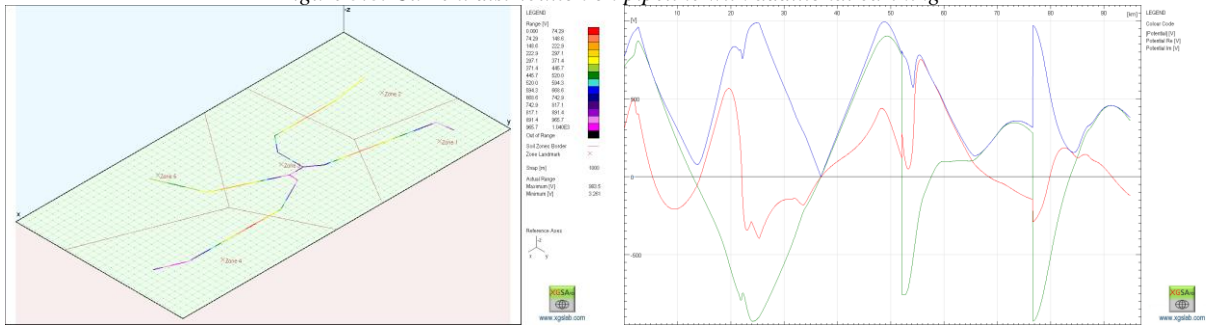


Figure 5.9: Potential distribution on pipeline with additional earthing

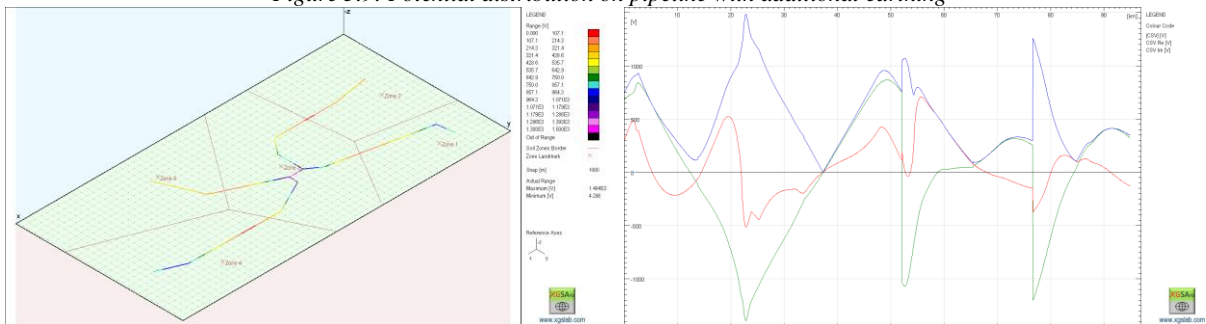


Figure 5.10: Covering stress voltage distribution on pipeline with additional earthing

Figure 5.11 represents the earth surface potential distribution in the interfering area. The effects of the substation is evident while the presence of pipelines and additional earthing is visible only far from the substation area.

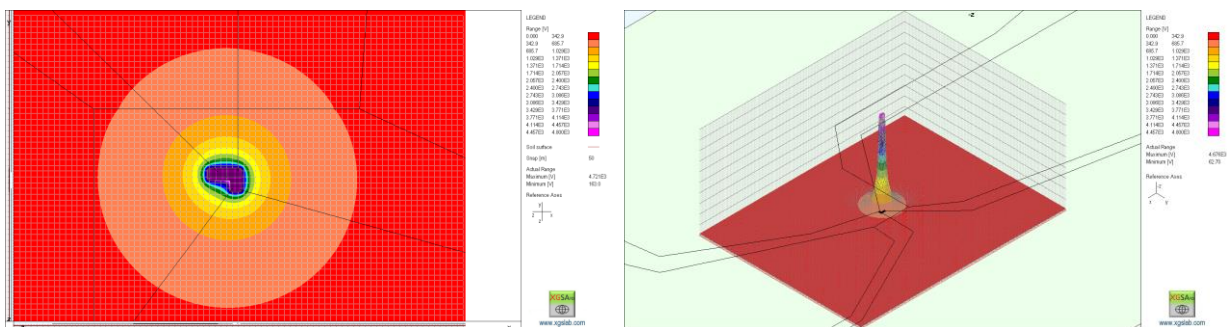


Figure 5.11: Earth surface potential distribution with additional earthing

6 - CONCLUSION

This paper describe the model implemented in a BEM based earthing software for electromagnetic simulations and a possible application at low frequency.

In particular this paper describes the electromagnetic interferences between a substation and four overhead power line and a buried steel pipeline network.

The interfering system is quite large and, as usual in similar conditions, it is supposed that the soil resistivity cannot be assumed as uniform. For this reason a multizone soil model has been used.

The cases study has been developed introducing some simplification about layout systems and fault current distributions, but in general conditions more complex and realistic scenarios may be simulated. The conductors network can include many conductors arranged and connected in an arbitrary way in the 3D space, the catenary disposal of aerial power lines can be used, aerial conductors can be single or bundled, the conductors network can be energized both with current or electromotive force, or with voltages induced by conductive, capacitive or inductive coupling and so on. Moreover the electric model of the system of conductors can include additional longitudinal or transversal impedance. The soil may be represented with a layered or with a multizone model.

All these options are made possible by the used hybrid model, and the accuracy of the results make the used software a very interesting design tools.

ACKNOWLEDGEMENTS

The authors wish to thank for the valuable tips all the anonymous reviewers of the previous submission.

BIBLIOGRAPHY

- [1] E.D. Sunde, *Earth Conduction Effects in Transmission Systems*, first ed., D. Van Nostrand Company Inc., New York, 1949.
- [2] S. Ramo, J.R. Whinnery, T. Van Duzer, *Fields and Waves in Communication Electronics*, first ed., Wiley International Edition, New York and London, 1965.
- [3] ITU / CCITT DIRECTIVES Volume III, Capacitive, inductive and conductive coupling: physical theory and calculation methods, Geneva (1989).
- [4] F.P. Dawalibi, R.D. Southey, Analysis of Electrical Interference from Power Lines to Gas Pipelines – Part I: Computation Methods, *IEEE Transactions on Power Delivery*, Vol. 4, No. 3, July 1989, pp. 1840 – 1846.
- [5] *Electro Magnetic Transient Program Theory Book*, Bonneville Power Administration, Portland, Oregon, 1995.
- [6] CIGRE WG 36.02 doc. 95 “Guide on Influence of High Voltage AC Power System an Metallic Pipelines” (1995).
- [7] L.D. Grcev, Computer analysis of Transient Voltages in Large Grounding Systems, *IEEE Transactions on Power Delivery*, Vol. 11, No. 2, April 1996, pp. 815 – 823.
- [8] R. Andolfato, L. Bernardi, L. Fellin, Aerial and Grounding System Analysis by the Shifting Complex Images Method, *IEEE Transactions on Power Delivery*, Vol. 15, No. 3, July 2000, pp. 1001 – 1009.
- [9] L.D. Grcev, V. Arnautovski Toseva, Grounding System Modeling for High Frequencies and Transient: Some Fundamental Considerations, *IEEE Power Tech Conference Proceedings*, Bologna (2003).
- [10] CIGRE WG C4.501 doc. 543 “Guide for Numerical Electromagnetic Alaysist Method and its Appliction to Surge Phenomena” (June 2013).
- [11] D. Cavka, N. Mora, F. Rachidi, A Comparison of Frequency Dependent Soil Models: Application to the Analysis of Grounding Systems, *IEEE Transactions on Electromagnetic Compatibility*, Vol. 56, No. 1, February 2014, pp. 177 – 187.
- [12] “XGSLab rel. 6.5.3 User’s Guide” SINT Ingegneria Srl - Italy.
- [13] “XGSLab rel. 6.5.3 Tutorial” SINT Ingegneria Srl - Italy.